ELSEVIER

Journal of Chromatography B, 752 (2001) 233–245

JOURNAL OF CHROMATOGRAPHY B

www.elsevier.com/locate/chromb

Identification of multiple sources of charge heterogeneity in a recombinant antibody

Reed J. Harris[a,*], Bruce Kabakoff[b], Frank D. Macchi[a], Felicity J. Shen[a], May Kwong[a], James D. Andya[c], Steven J. Shire[c], Nancy Bjork[a], Klara Totpal[b], Anthony B. Chen[b]

[a]*Analytical Chemistry Department, Genentech Inc., 1 DNA Way, South San Francisco, CA 94080, USA*
[b]*Quality Control Department, Genentech Inc., 1 DNA Way, South San Francisco, CA 94080, USA*
[c]*Pharmaceutical Research and Development Department, Genentech Inc., 1 DNA Way, South San Francisco, CA 94080, USA*

Abstract

Seven forms of a therapeutic recombinant antibody that binds to the *her2/neu* gene product were resolved by cation-exchange chromatography. Structural differences were assigned by peptide mapping and HIC after papain digestion. Deamidation of light chain asparagine 30 to aspartate in one or both light chains is responsible for two acidic forms. A low potency form is due to isomerization of heavy chain aspartate 102; the Asp102 succinimide is also present in a basic peak fraction. Forms with both Asn30 deamidation and Asp102 isomerization modifications were isolated. Deamidation of heavy chain Asn55 to isoaspartate was also detected. Isoelectric focusing in a polyacrylamide gel was used to verify the assignments. All modifications were found in complementarity determining regions.

Keywords: Charge heterogeneity; Peptide mapping; Recombinant antibody

1. Introduction

The general structural features of immunoglobulins have been known for decades, including the complete amino acid sequence and disulfide bonding pattern for IgG_1 [1] as well as the typical N-linked oligosaccharides found at a conserved position in the C_H2 domain [2]. For recombinant monoclonal antibodies whose light chain and heavy chain sequences are known in advance of any chemical characterization, there would appear to be little potential for the discovery of novel or interesting features, particularly for a large molecule with four polypeptide chains. However, a number of reports are now available detailing variations of covalent structure that introduce undesirable properties, including methionine oxidation that affects the potency and stability of OKT3 [3], a mutation unintentionally introduced during transfection [4], glycosylation differences that influence F_c effector functions [5], or antibody fragmentation [6]. Assays for the determination of the extent of overall deamidation [7], the types of N-linked oligosaccharides [8], or the extent of heavy chain glycosylation [9] are available. The processing of C-terminal lysine residues from antibody heavy chains has been noted by

*Corresponding author. Tel.: +1-650-225-4187; fax: +1-650-225-3554.
E-mail address: reed@gene.com (R.J. Harris).

0378-4347/01/$ – see front matter
PII: S0378-4347(00)00548-X

many [10], but this is not a significant issue except that it introduces charge heterogeneity that can mask other structural variants.

The remaining challenge for the analytical chemist is to resolve minor forms, determine the structural features that distinguish them from the major form, and to assign their potency or pharmacokinetic properties. This task is complicated for monoclonal antibodies by the dimeric nature of the molecule, since often only one light or heavy chain is affected, and by the overall size (approximately 148 kDa). A number of analytical approaches have been described, including peptide mapping [3,4,11], mass spectrometry [12,13], hydrophobic interaction chromatography [14–16], capillary electrophoresis [9], and cation exchange after papain digestion [17]. Approval by regulatory authorities for therapeutic recombinant antibodies requires the development of methods that can show key structural features, particularly those that reveal instability that could affect potency or pharmacokinetic aspects. In addition, such methods often have value for formulation development and/or in the assignment of product expiration dating [18].

rhuMAb HER2 (Herceptin®, trastuzumab for injection) has been licensed for the treatment of metastatic breast cancer involving over-expression of the *her2/neu* gene [19]. In unpublished studies with muMAb 4D5, the murine monoclonal anti-$p185^{her2/neu}$ antibody [20] that is the parent of the humanized antibody (rhuMAb HER2), we found that light chain Asn30 was prone to deamidation when stored at elevated temperatures in a pH 7.4 phosphate-buffered saline (PBS) excipient; this residue was part of a muMAb 4D5 light chain CDR segment that was transferred to the humanized antibody [21]. Subsequent studies with rhuMAb HER2 showed that a succinimide accumulated at the heavy chain Asp102 position when the humanized antibody was incubated at pH 5 in an acetate-NaCl buffer [14]. We investigated the possibility that cation-exchange chromatography could serve as a single analytical method that would allow monitoring of Asn30 deamidation and Asp102 succinimide formation. In addition to these known charge variants, four other minor peak fractions were isolated by cation-exchange chromatography and characterized.

The cation-exchange method described in this paper is the validated method used for the release of rhuMAb HER2 production lots. Seven forms can be resolved by cation-exchange chromatography. All were assigned using a variety of analytical methods, including trypsin and endoproteinase Asp-N peptide map analyses, hydrophobic interaction chromatography (HIC) after papain digestion, isoelectric focusing in a polyacrylamide gel (IEF), and sequential Edman degradation after alkaline hydroxylamine cleavage. Assignment of peptide fractions required sequential Edman degradation and MALDI–TOF mass spectrometry. The potencies of three forms were determined using an assay that measures the ability of rhuMAb HER2 to inhibit proliferation of a human breast carcinoma (BT-474) cell line that over-expresses the *her2/neu* gene.

2. Methods

2.1. Materials

Most rhuMAb HER2 samples were formulated at 25 mg/ml in 5 m*M* histidine, pH 6, 60 m*M* trehalose and 0.01% polysorbate 20. Accelerated degradation samples from an earlier clinical production process were incubated for 90 days at 30°C (degraded) or 2–8°C (control) in 5 m*M* NaOAc, pH 5, 145 m*M* NaCl and 0.01% polysorbate 20 to enrich for minor structural variants that are found in trace quantities in current production material.

2.2. Cation-exchange chromatography

A 4.6×250 mm analytical BakerBond CSX column was equilibrated for 20 min with 90% buffer A (20 m*M* sodium phosphate, pH 6.9) and 10% buffer B (20 m*M* sodium phosphate, pH 6.9, with 200 m*M* NaCl) at a 2 ml/min flow-rate, then the flow-rate was reduced to 1 ml/min. The column temperature was maintained at 40°C. Upon sample injection, a linear gradient changing from 10 to 45% buffer B over 55 min was begun. The column was washed with 100% buffer B at 2 ml/min for 5 min, then re-equilibrated with 10% buffer B. The column effluent was monitored at 280 and 214 nm.

Peak fractions were collected manually and pooled from multiple 2.5 mg injections for analysis using

the procedure(s) described below. The IEX-C peak fraction was collected from the accelerated degradation (30°C) sample, then exchanged by dialysis into pH 7.4 PBS for incubation at ambient temperature for 36 h.

2.3. Tryptic peptide map analysis

S-carboxymethylation was performed prior to digestion with trypsin. Samples were exchanged by dialysis into a pH 8.6 buffer containing 6 *M* guanidine, 0.36 *M* Tris and 1 m*M* EDTA. Dithiothreitol (DTT; Sigma) was added to a final concentration of 10 m*M* and the samples were incubated at 37°C for 1 h. Iodoacetic acid (Sigma), freshly prepared in 2.9 *M* NaOH, was then added to a concentration of 35 m*M*. After a 15-min incubation at 37°C in the dark, the alkylation was quenched by adding dithiothreitol to a final concentration of 40 m*M*.

The reduced and *S*-carboxymethylated samples were then exchanged by dialysis into a pH 7.5 buffer containing 10 m*M* Tris and 0.1 m*M* $CaCl_2$. TPCK-treated trypsin (Worthington) was added to the samples at a 1:40 (w:w HER2) ratio. Digestion was allowed to proceed for 4 h at 37°C, then trifluoroacetic acid (TFA; Pierce) was added to bring the samples to 0.5% TFA by volume.

Reversed-phase HPLC (RP-HPLC) was performed using a Hewlett-Packard 1090M HPLC system equipped with a Vydac C18 (4.6×250 mm) column; solvents A and B were 0.1% TFA in water and 0.1% TFA in acetonitrile, respectively. The column was equilibrated at a flow-rate of 1 ml/min with 100% solvent A at 30°C. A period of 3 min after injection of trypsin-digested material, a linear gradient was developed from 0 to 40% solvent B in 80 min. Peak fractions were collected manually.

2.4. Asp-N peptide map analysis

Samples were *S*-carboxymethylated as described above, then exchanged by dialysis into a pH 8 buffer containing 100 m*M* NaOAc, 10 m*M* Tris and 1 m*M* $CaCl_2$. Endoproteinase Asp-N (Boehringer Mannheim) was added at a 1:200 (w:w HER2) ratio, and digestion was allowed to proceed for 3 h at 37°C; a second 1:200 aliquot was then added for another 3 h digestion at 37°C.

RP-HPLC was performed using a Hewlett-Packard 1090M HPLC system equipped with a Vydac C18 (2.1×250 mm) column; solvents A and B were 0.1% TFA in water and 0.1% TFA in acetonitrile, respectively. The column was equilibrated at a flow-rate of 0.25 ml/min with 100% solvent A at 30°C. Three min after sample injection, a linear gradient was developed from 0 to 50% solvent B in 75 min. Peak fractions were collected manually.

2.5. Peptide analyses

Peptide identities for the collected peak fractions were assigned by either a comparison of masses obtained by matrix-assisted laser desorption ionization time-of-flight mass spectrometry (MALDI–TOF/MS) with the expected peptide masses, or by sequential Edman degradation. MALDI–TOF/MS samples were crystallized in a 10% 2′,4′,6′-trihydroxyacetophenone matrix containing 25% acetonitrile and 75% 13.3 m*M* ammonium citrate. MALDI–TOF/MS positive-ion spectra were obtained using a PerSeptive Biosystems Voyager Elite instrument. Edman degradation was performed using ABI 477A/120, ABI 494 or Hewlett-Packard G1000A sequencers, with quantitation by relative peak height comparisons to external PTH-standard mixtures.

2.6. Papain/HIC analysis

Samples were exchanged into 135 m*M* Tris, pH 7.2, 2 m*M* EDTA and 10 m*M* cysteine. Papain (Boehringer Mannheim) was added at a 1:200 (w:w HER2) ratio, and digestion was allowed to proceed for 2 h at 37°C, then a second 1:200 aliquot was added for another 2 h digestion. A Hewlett-Packard HP1090 system, equipped with a TosoHaas 4.6×35 mm NPR-butyl column, was operated with a 1 ml/min flow-rate and a column temperature of 30°C. Solvent A was 2 *M* ammonium sulfate containing 20 m*M* Tris, pH 7, while solvent B contained only 20 m*M* Tris, pH 7. Papain fragments were eluted using a 34 min linear gradient from 10 to 100% solvent B.

2.7. Alkaline hydroxylamine cleavage

Samples from the main cation-exchange peak (IEX-3) and the IEX-C peak were exchanged into 2 *M* hydroxylamine and 0.2 *M* Tris, pH 9, for a 2-h incubation at 40°C. The samples were then loaded onto the reversed-phase support of a Hewlett-Packard G1000A protein sequencer, and analyzed using Edman degradation chemistry version 3.1.

2.8. Isoelectric focusing in a polyacrylamide gel

An isoelectric focusing polyacrylamide gel, containing 3.9% acrylamide/bis (Pharmacia PlusOne Ready Mix IEF, 30% [w/v] stock solution), 0.5% Triton X-100, 0.17% pH 3.5–10 ampholines, 0.94% pH 8–9.5 ampholines, and 0.88% pH 9–11 ampholines (all Pharmacia), was degassed and cast vertically with 0.75 mm spacers on a GelBond PAG film (Pharmacia). The gel was prefocused at 4°C on a LKB 2217 Ultraphor IEF apparatus at 400 V, 100 mA, and 5 W for 9 min with 1 N sodium hydroxide and 0.4 *M* HEPES for the cathode and anode.

Samples were concentrated using Amicon Centricon-30 units prior to loading the gel. Samples and p*I* markers (Pharmacia) were loaded on paper applicator strips 2 cm from the anode. The voltage limit was increased to 450 V, 120 mA and 5 W after loading the samples. The voltage limit was gradually increased over 25 min to 900 V, 120 mA and 7 W. After 60 min of gel focusing, the voltage was increased to 1150 V to continue focusing for an additional 120 min.

The focused gel was fixed in a 10% trichloroacetic acid, 5% sulfosalicyclic acid (w/v) solution for 45 min, washed twice for 20 min each in a 20% ethanol, 6.25% acetic acid solution, then stained in 0.125% Coomassie R-250, 0.05% Cu_2SO_4, 37.5% ethanol for 90 min. A 45-min intermediate destain of 0.5% Cu_2SO_4, 7.5% acetic acid, 40% MeOH was used to help clear the background. Finally the gel was destained in 20% EtOH/6.25% acetic acid until a clear background was obtained. The destained gel was dried onto the attached gel backing.

2.9. BT-474 cell proliferation assay

BT-474 human breast carcinoma cells (ATCC HTB 20) were grown in DMEM:F12 (1:1) medium (Gibco) supplemented with 10% fetal bovine serum (HyClone) and 2 m*M* glutamine. BT-474 cell suspensions of 1×10^5 per-ml were made; 100 μl were dispensed per-well in Costar 96-well tissue culture plates, and then preincubated for 1–3 h at 37°C. A total of 100 μl of samples and standards of varying concentrations were added and incubated for 5 days at 37°C. At the end of the incubation, the cell number was quantitated after adding alamarBlue™ (AccuMed International). AlamarBlue™ is a redox dye that fluoresces when reduced by live cells. Relative fluorescence (530 nm excitation, 590 nm emission) was measured using a Cambridge Technology Model 7620 plate reader. A 4-parameter logistic curve-fitting program was used to generate a standard curve that reports the rhuMAb HER2 concentration. Specific activity was relative to the antiproliferative activity of the reference lot (assigned 100% specific activity).

3. Results

The primary sequences and complementarity-determining regions (CDRs) of the rhuMAb HER2 light and heavy chain genes are given in Fig. 1. These sequences are based on the structure proposed after humanization of the murine antibody [21], and were verified by assignment of peptide fractions obtained after tryptic digestion [4]. The heavy chain C-terminal Lys450 residue is not shown for this sequence because it is removed from >99% of heavy chains, presumably by the action of basic carboxypeptidases [24], during cell culture production. The cation-exchange profile for rhuMAb HER2 is given in Fig. 2. The major peaks are numbered (1–4) while the less abundant forms are labeled with letters (A, B, C).

3.1. Assignment of IEX-1

A comparison of tryptic peptide maps obtained for IEX-1 and IEX-3 is given in Fig. 3, with peptide assignments for the collected peak fractions given in Table 1. IEX-1 gave two forms of the LC:25-42 peptide, with Asp (peak D30) or Asn (peak N30) at the Asn30 position, consistent with an underlying structure with one deamidated (Asp30) light chain and one light chain with the expected Asn30 se-

Light chain

```
1                   15                  30                  45
D I Q M T Q S P S S L S A S V G D R V T I T C R A S Q D V N T A V A W Y Q Q K P G K A P K

46                  60                  75                  90
L L I Y S A S F L Y S G V P S R F S G S R S G T D F T L T I S S L Q P E D F A T Y Y C Q Q

91                  105                 120                 135
H Y T T P P T F G Q G T K V E I K R T V A A P S V F I F P P S D E Q L K S G T A S V V C L

136                 150                 165                 180
L N N F Y P R E A K V Q W K V D N A L Q S G N S Q E S V T E Q D S K D S T Y S L S S T L T

181                 195                 210  214
L S K A D Y E K H K V Y A C E V T H Q G L S S P V T K S F N R G E C
```

Heavy chain

```
1                   15                  30                  45
E V Q L V E S G G G L V Q P G G S L R L S C A A S G F N I K D T Y I H W V R Q A P G K G L

46                  60                  75                  90
E W V A R I Y P T N G Y T R Y A D S V K G R F T I S A D T S K N T A Y L Q M N S L R A E D

91                  105                 120                 135
T A V Y Y C S R W G G D G F Y A M D Y W G Q G T L V T V S S A S T K G P S V F P L A P S S

136                 150                 165                 180
K S T S G G T A A L G C L V K D Y F P E P V T V S W N S G A L T S G V H T F P A V L Q S S

181                 195                 210                 225
G L Y S L S S V V T V P S S S L G T Q T Y I C N V N H K P S N T K V D K K V E P K S C D K

226                 240                 255                 270
T H T C P P C P A P E L L G G P S V F L F P P K P K D T L M I S R T P E V T C V V V D V S

271                 285                 300                 315
H E D P E V K F N W Y V D G V E V H N A K T K P R E E Q Y N S T Y R V V S V L T V L H Q D

316                 330                 345                 360
W L N G K E Y K C K V S N K A L P A P I E K T I S K A K G Q P R E P Q V Y T L P P S R E E

361                 375                 390                 405
M T K N Q V S L T C L V K G F Y P S D I A V E W E S N G Q P E N N Y K T T P P V L D S D G

406                 420                 435                 449
S F F L Y S K L T V D K S R W Q Q G N V F S C S V M H E A L H N H Y T Q K S L S L S P G
```

Fig. 1. Primary sequences of the rhuMAb HER2 light and heavy chains. The heavy chain Asn300 glycosylation site is underlined. Complementarity-determining regions are indicated by the boldface italicized type.

quence. The main peak fraction (IEX-3) shows only the Asn30 form of the LC:25-42 peptide.

The expected deamidation of proteins and peptides proceeds via a succinimide intermediate, followed by partial hydrolysis of the succinimide ring to produce isoaspartate (the major product) and aspartate (the minor product) [22,23]. The Asn30 deamidation product is aspartate, not isoaspartate, indicating that this reaction does not proceed via the succinimide intermediate; an alternative mechanism, such as nucleophilic attack, may be responsible. The elution position of the LC:25-42 tryptic peptide with isoaspartate at the Asn30 position has been established. This isoAsp30 form is not present in the current production samples, but can be detected in an accelerated degradation sample where the material was held at 30°C for 90 days in a pH 5 acetate/saline liquid formulation (peak I30 in Fig. 4). In the pH 5 accelerated degradation samples, the IEX-1 form converts to the IEX-3 elution position (data not shown).

HIC analysis after papain digestion was also performed, with papain cleaving the heavy chains between His227 and Thr228, producing two F_{ab} fragments (each containing one light chain and one heavy chain 1-227 fragment) and one dimeric F_c

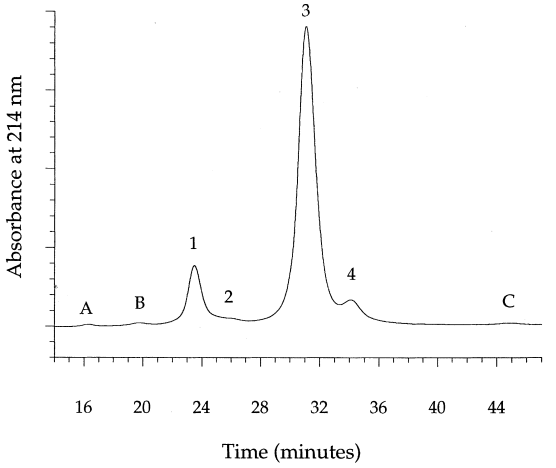

Fig. 2. rhuMAb HER2 cation-exchange profile. Peak assignments are given in Table 6.

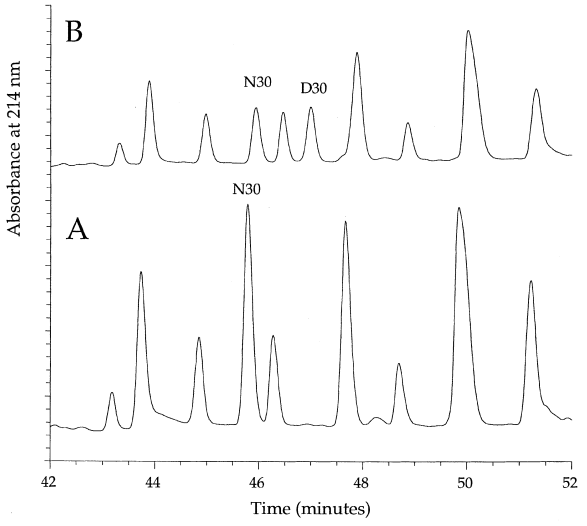

Fig. 3. Tryptic peptide map detail for (A) IEX-3 and (B) IEX-1. Labeled peak assignments are given in Table 1.

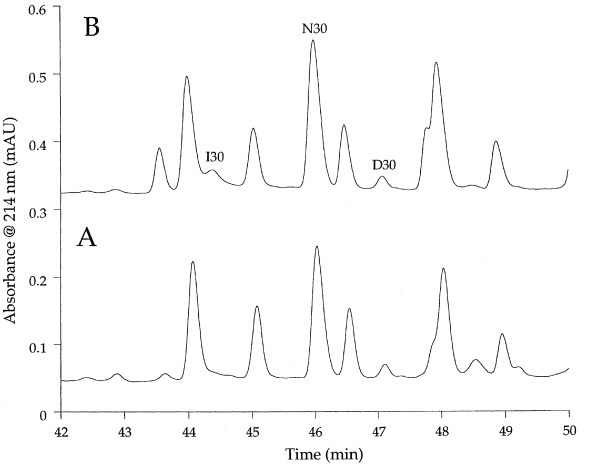

Fig. 4. Tryptic peptide map detail for stability samples. (A) control (2–8°C) sample. (B) sample stored at 30°C for 90 days in a pH 5 acetate-NaCl excipient.

(heavy chain 228-449) fragment. Analysis of IEX-1 by HIC after papain digestion shows two F_{ab} forms, one that elutes in the Asn30 position (HIC-III of Fig. 5), and a new peak that represents the Asp30 F_{ab} form (HIC-II of Fig. 5). IEX-1 also appears to be more acidic by IEF analysis (Fig. 6).

3.2. Assignment of IEX-C

The assignment of peak C was performed using material collected from the accelerated degradation study. Edman sequence analysis after alkaline hydroxylamine cleavage of the heavy chain indicated the position of the Asp102 succinimide in the IEX-C fraction [14]. The results, summarized in Table 2, show evidence of internal cleavage of the heavy chain between Asp102 and Gly103 only in IEX-C material, consistent with the presence of a succinimide at the Asp102 position of one heavy chain.

Table 1
Assignment of LC:25-42 peptides

Peak[a]	Observed Mass (Da)	Peptide sequence[b]	Assignment
I30	1991.2	ASQDVntavawyqqkpgk	LC:25-42, isoAsp30
N30	1990.0	ASQDVNTAVAWYQQKPGK	LC:25-42, Asn30
D30	1991.0	ASQDVDTAVAWYQQKPGK	LC:25-42, Asp30

[a] Peak identifiers refer to labels in Figs. 3 and 4.
[b] Lower case letters refer to residues not observed by Edman sequence analysis.

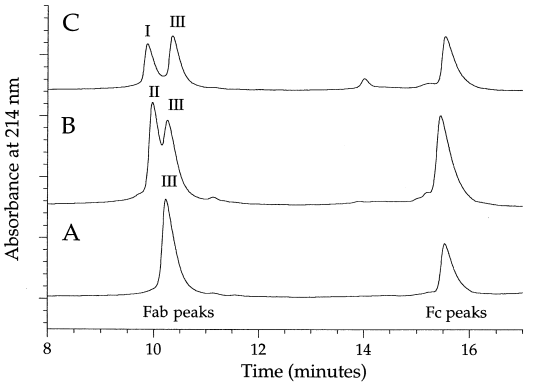

Fig. 5. Hydrophobic interaction chromatography after papain digestion of material collected by cation exchange. Approximately 20 μg were injected. (A) IEX-3. (B) IEX-1. (C) IEX-4.

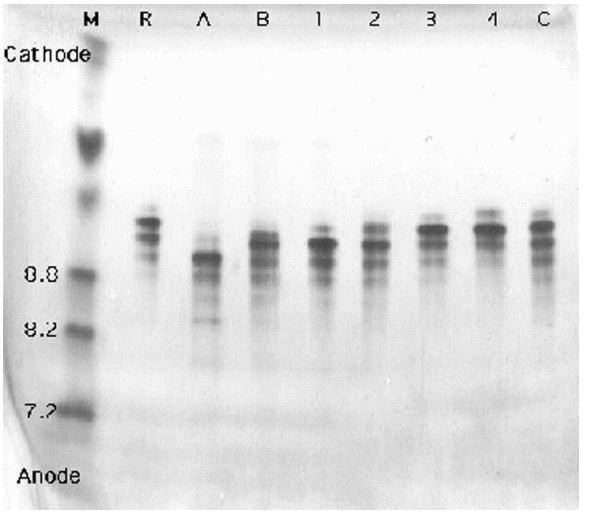

Fig. 6. Isoelectric focusing in a polyacrylamide gel. Approximately 5 μg of each cation-exchange fraction were loaded. Approximate p*I* values for the standards are given at the left. (M) IEF standards. (R) unfractionated rhuMAb HER2. (A) IEX-A. (B) IEX-B. (1) IEX-1. (2) IEX-2. (3) IEX-3. (4) IEX-4. (C) IEX-C.

Table 2
Sequence analysis after alkaline hydroxylamine cleavage

Peak	Observed sequences	nmol yield	Starting residue
IEX-3	DIQMTQSPSS	0.41	LC: 1–
	EVQLVESGGG	0.56	HC: 1–
IEX-C	DIQMTQSPSS	0.22	LC: 1–
	EVQLVESGGG	0.22	HC: 1–
	GFYAMDYWGQ	0.06	HC: 103–

For IEX-C, the yield of the internal sequence starting at Gly103 was about 25% of the overall heavy chain sequence yield, indicating approximately 50% cleavage of one heavy chain. The IEX-3 control sample was not susceptible to this internal cleavage by hydroxylamine. The IEX-C form is apparently more basic than the main peak form because the negative charge found on the Asp102 side-chain has been neutralized in the succinimide form.

Succinimides are typically unstable at neutral or alkaline pH [22,23,25]; as a result, the collected IEX-C material was already partially degraded upon collection, with the IEX-C form representing 83% of the total peak area (Fig. 7C). Further degradation of collected IEX-C material by incubation in phosphate buffered saline is demonstrated in Fig. 7B. The principal degradation products are IEX-4 and IEX-3, consistent with the known hydrolytic degradation pathway for protein succinimides, in which the major hydrolysis product is isoaspartate (represented by IEX-4) and the minor hydrolysis product is aspartate (represented by IEX-3). Trace amounts of the IEX-1 and IEX-2 forms also develop upon incubation in PBS (Fig. 7B), due to deamidation of light chain Asn30 as discussed below.

The instability of IEX-C in slightly alkaline conditions may also be responsible for the observation that IEX-3 and IEX-4 appear at the same

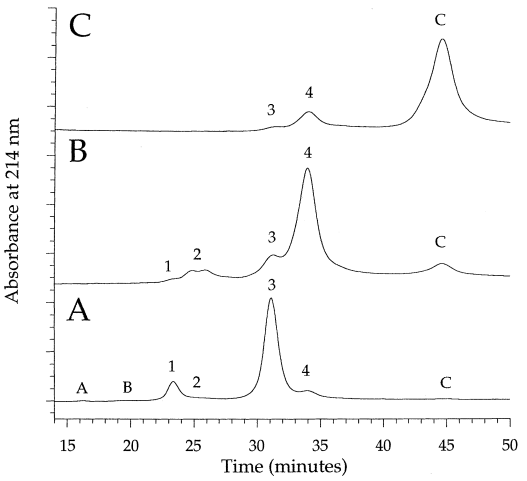

Fig. 7. Cation-exchange chromatography of (A) unfractionated rhuMAb HER2, (B) IEX-C material incubated for 36 h in PBS at 25°C, or (C) IEX-C −20°C control.

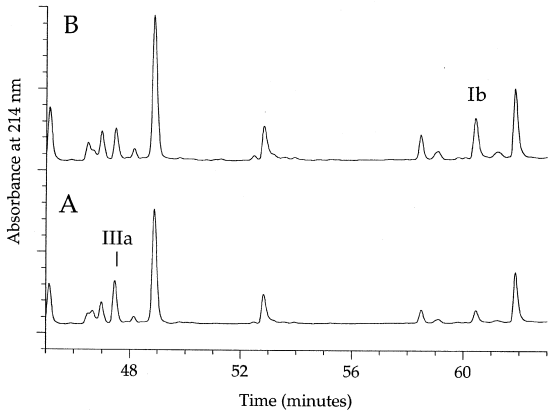

Fig. 8. Endoproteinase Asp-N digestion of F_{ab} peaks collected by HIC after papain digestion of IEX-4. (A) F_{ab}-III (Asp102). (B) F_{ab}-I (isoAsp102).

position in the IEF gel (Fig. 6), with the succinimide degrading under the alkaline pH conditions used for loading the samples and/or running the gel. We have not tested this hypothesis, so it may also be possible that the p*I* differences between the IEX-3 and IEX-4 forms are insufficient for IEF resolution.

3.3. Assignment of IEX-4

The presence of isoAsp102 in one heavy chain of IEX-4 was first indicated by the conversion of IEX-C primarily to the IEX-4 position after incubation in PBS as described above (Fig. 7B). To confirm this assignment, HIC after papain digestion was used to resolve the IEX-4 F_{ab} fragments; these appear as two equal peaks, with F_{ab}-III eluting in the same position as the IEX-3 F_{ab} peak (Asp102) and F_{ab}-I eluting earlier (Fig. 5C).

No differences were observed when the tryptic peptide maps of the F_{ab} forms I and III were compared (data not shown). In our experience, endoproteinase Asp-N digestion has been useful to distinguish aspartyl from isoaspartyl residues based on the relatively high resistance of the isoaspartyl form to Asp-N digestion. The Asp-N digest maps of F_{ab} peaks I and III are given in Fig. 8, with peptide assignments given in Table 3. In Fig. 8A, F_{ab}-III released primarily the HC:90-102 peptide (peak IIIa), consistent with cleavage at Asp102. In Fig. 8B, F_{ab}-I released primarily the HC:90-107 peptide (peak Ib), consistent with poor cleavage at isoAsp102. Confirmation of the isoAsp102 assignment for peak Ib was achieved by sequential Edman degradation, showing a complete loss of sequencing yield after Gly101 of the peptide sequence, indicating the presence of an isoaspartate residue at position 102 [26]. The Asp102–Met107 peptide was not detected in either Asp-N map.

When a Lys450 residue is present on one heavy chain, such a rhuMAb HER2 form will also elute in the IEX-4 position (data not shown). The samples used to perform the studies described in this report did not contain any heavy chain Lys450 residues, but this type of interfering co-elution can easily be eliminated by pre-incubation with carboxypeptidase B [15].

3.4. Assignment of IEX-2

The poorly resolved IEX-2 peak pair was collected from the control sample as a single fraction. The tryptic peptide map of IEX-2 shows a mixture of the Asn30 and Asp30 forms of the LC:25-42 peptide (Fig. 9D), at approximately a 2:1 ratio. The papain/HIC profile for IEX-2 shows the three known F_{ab} forms (Fig. 10D), including the isomerized (Asn30/isoAsp102) F_{ab} found in HIC-I, the deamidated (Asp30/Asp102) F_{ab} found in HIC-II, and the main F_{ab} form (Asn30/Asp102) found in the HIC-III position. As described above, thermal degradation of

Table 3
Assignment of Asp-N peptides from F_{ab}-I and F_{ab}-III (Fig. 8)

Peak	Observed mass (Da)	Peptide sequence[a]	Assignment
Ib	2120.3	DTAVYYCSRWGGdgfyam	HC: 90-107, isoAsp102
IIIa	1435.3	DTAVYYCSRWGG	HC: 90-101

[a] Lower case letters refer to residues not observed by Edman sequence analysis.

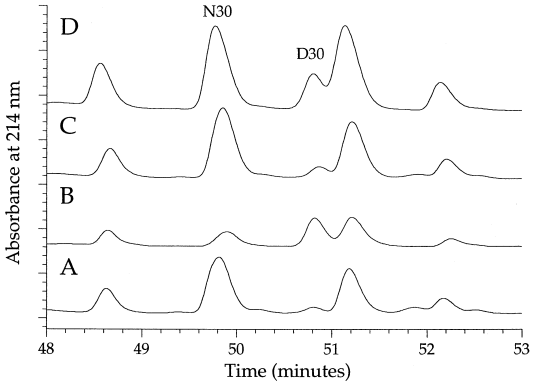

Fig. 9. Tryptic peptide map detail for cation-exchange peak fractions A, B and 2. D30 and N30 refer to the residue found at position 30 of the LC:25-42 peptide. (A) unfractionated rhuMAb HER2. (B) IEX-A. (C) IEX-B. (D) IEX-2.

the fraction containing the Asp102 succinimide (IEX-C) gave rise to a small amount of both forms of IEX-2 (Fig. 7B). The IEX-2 fraction appears in the same position in the IEF gel as IEX-1, both of which are more acidic than the main (IEX-3) form (Fig. 6).

The combined data suggest that the IEX-2 peaks represent forms of the rhuMAb HER2 antibody with both the Asp30 and isoAsp102 residue differences, though both are not necessarily in the same F_{ab}. The presence of IEX-2 as a peak pair after degradation of the IEX-C (succinimide) form (Fig. 7B) suggests that two slightly different antibody types are formed,

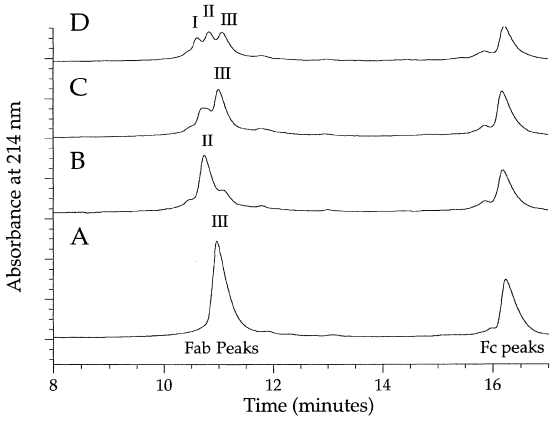

Fig. 10. Hydrophobic interaction chromatography after papain digestion of material collected by cation exchange. (A) IEX-3. (B) IEX-A. (C) IEX-B. (D) IEX-2.

each containing one deamidated Asp30 residue and one isoAsp102 residue.

Each rhuMAb HER2 molecule contains two F_{ab} regions. Papain digestion of rhuMAb HER2 forms with the Asp30 and isoAsp102 residues each found in *separate* F_{ab} regions would generate both the HIC-I (Asn30/isoAsp102) and HIC-II (Asp30/Asp102) forms. rhuMAb HER2 forms with both these modified residues (Asp30 and isoAsp102) in the *same* F_{ab} region would release the unmodified HIC-III form (Asn30/Asp102) and a new form (Asp30/isoAsp102) that might elute in yet a different position. The pattern observed for IEX-2 after papain digestion is consistent with this model (Fig. 10D), as the three known F_{ab} forms are observed in roughly equal amounts. Assuming deamidation and isomerization occur independently, the F_{ab} form containing both modifications (Asp30/isoAsp102) should also be present, but this form was not detected.

3.5. Assignment of IEX-A

Tryptic peptide mapping of IEX-A material shows primarily the Asp30 form of the LC:25-42 peptide (Fig. 9B). IEF analysis of this fraction shows that IEX-A is more acidic than the IEX-1 material (Fig. 6), at a position shifted twice the distance observed between IEX-3 and IEX-1. Papain/HIC analysis shows that this fraction contains mainly the Asp30 form of the F_{ab} (peak II in Fig. 10B). These results are consistent with IEX-A representing the form with two deamidated (Asp30) light chains.

3.6. Assignment of IEX-B

Tryptic peptide mapping of IEX-B material (Fig. 9C) shows the Asn30 and Asp30 forms of the LC:25-42 peptide in approximately the same ratios as the unfractionated sample (Fig. 9A). IEF analysis of this fraction shows that IEX-B is no more acidic than the IEX-1 material (Fig. 6). Papain/HIC analysis shows that this fraction contains a mixture of the Asn30 form of the F_{ab} (peak III in Fig. 10C) and a new, broad F_{ab} peak form. These results suggest the presence of an acidic modification that is different from those described above.

Asp-N peptide mapping of IEX-B material showed

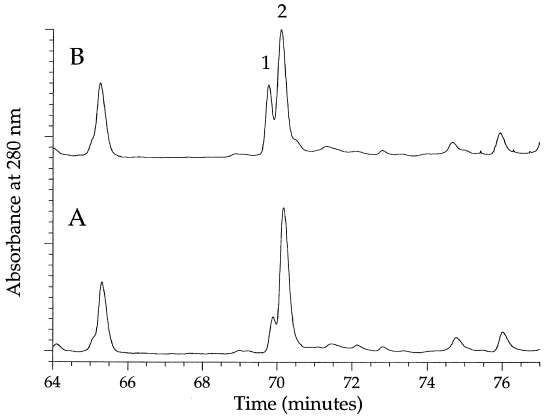

Fig. 11. Endoproteinase Asp-N peptide map detail. Peptide assignments for the labeled peaks are given in Table 4. (A) IEX-3. (B) IEX-B.

enrichment of peak B1 when compared to the IEX-3 control digestion pattern (Fig. 11). Peptide assignments are summarized in Table 4. Peak B1 contains a peptide with the HC:31-61 sequence (DTYIHWVRQAPGKGLEWVARIYPTNGYTRYA), but with a mass that is 1 Da higher than the B2 form of the HC:31-61 peptide obtained for the IEX-3 profile, consistent with the conversion of an Asn residue to Asp or isoAsp. Deamidation of Asn55 to Asp would give the same +1 Da mass difference, but is deemed unlikely because an Asp55 residue would be susceptible to Asp-N digestion. There was insufficient material to assign the deamidation site directly by sequencing techniques, but the only likely deamidation site in this peptide is found at Asn55 (in the Asn–Gly sequence underlined above), so the principal structural difference between IEX-B and IEX-3 was attributed to deamidation of Asn55 to isoaspartate.

Table 5
Relative potencies of IEX fractions in the BT-474 antiproliferation assay

Sample	Specific activity (%)
Unfractionated	100[a]
IEX-1	98
IEX-3	141
IEX-4	12-30[b]

[a] The reference material is assigned 100% potency.
[b] Curves did not dilute in parallel with the standard.

3.7. Potency determinations

In Table 5, the unfractionated rhuMAb HER2 reference standard is assigned a relative antiproliferative activity of 100%. The main peak (IEX-3) activity is higher for the main peak (141%). The deamidated material found in IEX-1 has the same activity as the unfractionated material (98%), but this is only 70% as potent as the main peak material. Material collected as IEX-4 is very low in potency, estimated at 12–30% relative antiproliferative activity (9–21% as potent as the main peak material); the exact potency could not be assigned for this fraction because the data curve did not dilute in parallel with the reference standard.

4. Discussion

Seven forms of rhuMAb HER2 can be resolved by cation-exchange chromatography (Table 6). All six minor forms could be assigned using a combination of analytical techniques, but in general, the data supporting the assignments of the peak fractions are easier to interpret for the more abundant forms. Asn30 is present as aspartate in an Asn–Thr se-

Table 4
Assignment of Asp-N peptides from IEX-3 and IEX-B

Peak	Observed mass (Da)	Peptide sequence[a]	Assignment
B1	3681.8	DTYIHWVRQAPGKGLEWVARIYPTXGYTRA	HC: 31-61, isoAsp55
B2	3680.8	DTYIHWVRQAPGKGLEWVARIYPTNGYTRA	HC: 31-61, Asn55

[a] The letter X refers to isoaspartate.

Table 6
rhuMab HER2 cation-exchange peak assignments

Peak	Peak area %	Structural difference(s)	At LC Asn30	At HC Asn55	At HC Asp102
A	0.5	Deamidated (to Asp) at Asn30 of both light chains	Asp/Asp	Asn/Asn	Asp/Asp
B	1.1	Deamidated (to isoAsp) at Asn55 in one heavy chain	Asn/Asn	isoAsp/Asn	Asp/Asp
1	13.6	Deamidated (to Asp) at Asn30 of one light chain	Asn/Asp	Asn/Asn	Asp/Asp
2	1.7	Deamidated (to Asp) at Asn30 of one light chain, and isomerized (to isoAsp) at Asp102 of one heavy chain	Asn/Asp	Asn/Asn	Asp/isoAsp
3	73.8	Main peak form	Asn/Asn	Asn/Asn	Asp/Asp
4	8.5	Isomerized (to isoAsp) at Asp102 of one heavy chain	Asn/Asn	Asn/Asn	Asp/isoAsp
C	0.7	Succinimide (Asu) at Asp102 position of one heavy chain	Asn/Asn	Asn/Asn	Asp/Asu

quence in one light chain in the most abundant minor form (IEX-1). The potency of IEX-1 is slightly reduced (70% as active as the main peak form). However, even when ~15% of the product pool is represented by this form, this lower potency does not have a significant effect on the overall potency of the pool. Thus, it was not necessary to remove the IEX-1 form during product recovery. A form that is deamidated in both light chains is barely detectable as peak IEX-A.

Deamidation of asparagine residues usually proceeds via a succinimide intermediate, with the favored product of deamidation being isoaspartate [22,23]. Deamidation of Asn30 to isoaspartate was observed for the murine monoclonal antibody (muMAb 4D5) that is the parent of rhuMAb HER2, but for some reason that is not yet clear, the Asn30 residues of the humanized antibody (rhuMAb HER2) do not deamidate to isoAsp during cell culture production. It is possible that the hydrogen bonding or polypeptide bond angles are different between muMAb 4D5 and rhuMAb HER2, as these structural features are important determinants for protein deamidation [27].

Tryptic maps performed on unfractionated stability samples revealed an increase in the isoAsp30 form of the LC:25-42 peptide along with a slight decrease in the Asp30 form, indicating that although Asn30 residues are stable at pH 5, Asp30 residues will form the succinimide and ultimately will be converted to isoAsp during tryptic map sample preparation. Thus, Asn30 residues deamidate to Asp at neutral pH during cell culture production but appear to be stable at pH 5, whereas the Asp30 residues formed by this deamidation appear to be stable at neutral pH but are prone to succinimide-mediated isomerization to isoAsp at pH 5.

The discovery of stable succinimide structures in proteins is an increasingly common experience [25,28–31]. Formation of these succinimides appears to be favored when these proteins are incubated near pH 5. Assignment of the rhuMAb HER2 IEX-C form was performed previously using fractions isolated by a different hydrophobic interaction chromatography method [14]. This work was repeated using cation-exchange chromatographic fractions collected from a stability sample, and the presence of the succinimide at the heavy chain Asp102 position was confirmed.

Incubation of the IEX-C fraction at neutral pH revealed links to the IEX-4 (Asn30/isoAsp102) and IEX-2 (Asp30/isoAsp102) forms. Assignment of the IEX-4 form required peptide mapping after endoproteinase Asp-N digestion of F_{ab} fragments. The IEX-2 form was assigned after papain/HIC analysis, which showed the presence of all known F_{ab} forms, indicating that the IEX-2 forms contain a deamidated light chain and an isomerized heavy chain, with these two modifications in either the same or separate F_{ab} regions.

The IEX-B form is unrelated to the other forms resolved by cation-exchange chromatography, being due to conventional deamidation, with heavy chain Asn55 (found in an Asn–Gly sequence in a heavy chain CDR) converted to isoAsp. Additional minor charge heterogeneity that is not resolved by cation-exchange seems unlikely given that the peak assignments are consistent with the charge patterns observed by isoelectric focusing in a polyacrylamide gel.

The rhuMAb HER2 potency assay measures the

ability of the antibody to prevent the proliferation of a cell line derived from a human adenocarcinoma that over-expresses the *her2/neu* gene. The form with one deamidated light chain is only slightly reduced in potency, whereas the form with isoAsp102 in one heavy chain CDR is greatly affected. These potency differences are consistent with earlier studies that demonstrated that rhuMAb HER2 antiproliferative activity requires a bivalent antibody [32]. The other minor peak forms were not collected for potency determinations because they would not have much effect on the potency of the unfractionated pool given their relatively low abundance (Table 6).

The resolution offered by this technique is remarkable, with separations achieved between rhuMAb HER2 forms that differ at one or two positions in a 148 kDa protein. The resolution between Asp102/Asp102 (IEX-3) and Asp102/isoAsp102 (IEX-4) forms is particularly unusual, given the trivial difference in charge; this separation may be due to the isomerization changing the structure in such a way that the isoAsp-containing forms present a difference in surface charge features. The X-ray structure of rhuMAb HER2 shows that the Asp102–Tyr105 region is known to form an interface with light chain residues Phe53–Tyr55 [33], hence disruption of this interface could cause profound structural changes. The sharp reduction in potency for the IEX-4 form is consistent with this explanation.

A number of protein instability studies have proposed that ''hot spots'' exist for deamidation, particularly at Asn–Gly and Asn–Ser sequences [34,35]. Six Asn–Gly and Asn–Ser sequences are present in rhuMAb HER2 (not including the glycosylated heavy chain Asn300 site), yet only Asn55, found in an Asn–Gly sequence, is susceptible to deamidation. The major deamidation site at Asn30 is found in an Asn–Thr sequence.

The three labile residues (Asn55, Asn30 and Asp102) all are found at sites in complementarity-determining (CDR) regions. This suggests that for this antibody, surface accessibility and flexibility, both of which are relatively high in the CDR regions, is more predictive of polypeptide chain degradation sites than the primary sequence. These properties (surface accessibility and local flexibility) coincidentally improve prospects for developing a chromatographic purity assay where altered interactions between the antibody's surface features and a stationary phase are the basis for the separation. The same factors that contribute to chromatographic resolution might not be achieved with IEF methods. In the example of rhuMAb HER2, cation-exchange chromatography provided excellent resolution of several closely-related minor forms, ultimately allowing us to delineate structural features with meaningful biological consequences, such as lower potency.

Acknowledgements

The authors gratefully acknowledge the assistance of Edward Chin and Damon Papac with MALDI–TOF/MS analysis.

References

[1] G.M. Edelman, B.A. Cunningham, W.E. Gall, P.D. Gottleib, U. Rutishauser, M.Y. Waxdal, Proc. Natl. Acad. Sci. USA 63 (1969) 237.
[2] N. Takahasi, I. Ishii, H. Ishihara, M. Mori, S. Tejima, R. Jefferis, S. Endo, Y. Arata, Biochemistry 26 (1987) 1137.
[3] D.J. Kroon, A. Baldwin-Ferro, P. Lalan, Pharm. Res. 9 (1992) 1386.
[4] R.J. Harris, A.A. Murnane, S.L. Utter, K.L. Wagner, E.T. Cox, G.D. Polastri, J.C. Helder, M.B. Sliwkowski, Bio/Technol. 11 (1993) 1293.
[5] M.R. Lifely, C. Hale, S. Boyce, M.J. Keen, J. Phillips, Glycobiol. 5 (1995) 813.
[6] A.J. Alexander, D.E. Hughes, Anal. Chem. 67 (1995) 3626.
[7] P.K. Tsai, M.W. Bruner, J.I. Irwin, C.C. Yu Ip, C.N. Oliver, R.W. Nelson, D.B. Volkin, C.R. Middaugh, Pharm. Res. 10 (1993) 1580.
[8] D.I. Papac, J.B. Briggs, E.T. Chin, A.J.S. Jones, Glycobiol. 8 (1998) 445.
[9] G. Hunt, W. Nashabeh, Anal. Chem. 71 (1999) 2390.
[10] R.J. Harris, J. Chromatogr. B 705 (1995) 129.
[11] K. Kannan, M.G. Mulkerrin, M. Zhang, R. Gray, T. Steinharter, K. Sewerin, R. Baffi, R. Harris, C. Karunatilake, J. Pharm. Biomed. Anal. 16 (1997) 631.
[12] D.A. Lewis, A.W. Guzzetta, W.S. Hancock, M. Costello, Anal. Chem. 66 (1994) 585.
[13] G.D. Roberts, W.P. Johnson, S. Burman, K.R. Anumula, S.A. Carr, Anal. Chem. 67 (1995) 3613.
[14] M.Y. Kwong, R.J. Harris, Protein Sci. 3 (1994) 147.
[15] F.J. Shen, M.Y. Kwong, R.G. Keck, R.J. Harris, in: D.R. Marshak (Ed.), Techniques in Protein Chemistry VII, Academic Press, San Diego, 1996, p. 275.

[16] J. Cacia, R. Keck, L.G. Presta, J. Frenz, Biochemistry 35 (1996) 1897.
[17] K.G. Moorhouse, W. Nashabeh, J. Deveney, N.S. Bjork, M.G. Mulkerrin, T. Ryskamp, J. Pharm. Biomed. Anal. 16 (1997) 593.
[18] Y.J. Wang, R. Pearlman (Eds.), Stability and Characterization of Protein and Peptide Drugs, Plenum Press, New York, 1993.
[19] R.I. Cohen, Cancer Radiother. Radiopharm. 14 (1999) 1.
[20] B.M. Fendly, M. Winget, R.M. Hudziak, M.T. Lipari, M.A. Napier, A. Ullrich, Cancer Res. 50 (1990) 1550.
[21] P. Carter, L. Presta, C.M. Gorman, J.B.B. Ridgway, D. Henner, W.L.T. Wong, A.M. Rowland, C. Kotts, M.E. Carver, H.M. Shepard, Proc. Natl. Acad. Sci. USA 89 (1992) 4285.
[22] T. Geiger, S. Clarke, J. Biol. Chem. 262 (1987) 785.
[23] C. Oliyai, R. Borchardt, Pharm. Res. 10 (1993) 95.
[24] P. Rao, A. Williams, A. Baldwin-Ferro, E. Hanigan, D. Kroon, M. Makowski, E. Meyer, V. Numsuwan, E. Rubin, A. Tran, BioPharm. 4 (1991) 38.
[25] R. Bischoff, P. Lepage, M. Jaquinod, G. Cauet, M. Acker-Klein, D. Clesse, M. Laporte, A. Bayol, A. Van Dorsselaer, C. Roitsch, Biochemistry 32 (1993) 725.
[26] D.G. Smyth, W.H. Stein, S. Moore, J. Biol. Chem. 237 (1962) 1845.
[27] A.A. Kossiakoff, Science 240 (1988) 191.
[28] G. Teshima, J.T. Stults, V. Ling, E. Canova-Davis, J. Biol. Chem. 266 (1991) 13544.
[29] B.N. Violand, M.R. Schlittler, E.W. Kolodziej, P.C. Toren, M.A. Cabonce, N.R. Siegel, K.L. Duffin, J.F. Zobel, C.E. Smith, J.S. Tou, Protein Sci. 1 (1992) 1634.
[30] Z. Shahrokh, G. Eberlein, D. Buckley, M.V. Paranandi, D.W. Aswad, P. Stratton, R. Mischak, Y.J. Wang, Pharm. Res. 11 (1994) 936.
[31] H. Tomizawa, H. Yamada, T. Ueda, T. Imoto, Biochemistry 33 (1994) 8770.
[32] R.F. Kelley, M.P. O'Connell, L. Presta, C. Eigenbrot, M. Covarrubias, B. Snedecor, J.H. Bourell, D. Vetterlein, Biochemistry 31 (1992) 5434.
[33] C. Eigenbrot, M. Randal, L. Presta, P. Carter, A.A. Kossiakoff, J. Mol. Biol. 229 (1993) 969.
[34] T. Wright, Protein Eng. 4 (1991) 283.
[35] M. Powell et al., in: Y.J. Wang, R. Pearlman (Eds.), Formulation, Characterization and Stability of Protein Drugs: Case Histories, Pharmaceutical Biotechnology, Plenum Press, New York, 1996, p. 1, Chapter 1.